Journal of Applied Polymer Science

Research on the preparation and characterization of chitosan grafted polyvinylpyrrolidone gel membrane with iodine

Mingze Sai,[1] Rui Guo,[1] Lu Chen,[2] Ningning Xu,[1] Yang Tang,[1] Derun Ding[1]

[1]College of Chemistry and Chemical Engineering, Shanghai University of Engineering Science, Shanghai 201620, People's Republic of China

[2]Hubei Key Laboratory of Bioinorganic Chemistry & Materia Medica, School of Chemistry and Chemical Engineering, Huazhong University of Science and Technology, Wuhan 430074, People's Republic of China

Correspondence to: D. Ding (E-mail: dingderun@sues.edu.cn)

ABSTRACT: The chitosan grafted polyvinylpyrrolidone gel membrane with iodine (CS-PVP-I_2-G-M) was prepared by chitosan–polyvinylpyrrolidone–iodine complex liquid (CS-PVP-I_2-L) mixed with gelatin. The intermediate product CS-PVP-I_2-L was prepared by CS grafted PVP in the protection of N_2 with dimethyl 2,2′-azobis (2-methylpropionate) (AIBME) as initiator, then a certain amounts of iodine in ethanol solution was added. The properties of CS-PVP-I_2-G-M were characterized by IR, UV–Vis, SEM, XRD, DSC, and so forth. The iodine release results coherent with the release kinetic model—Fick diffusion laws, has a burst effect first, and then spread, and the emission of iodine was maintained within a certain range and kept at a stable level permanently, showed a sustained-release effect of iodine. The inhibition zone diameters of CS-PVP-I_2-G-M against *Staphylococcus aureus* and *Escherichia coli* were both greater than 16 mm, it demonstrated significant antibacterial activity. Double effects sustained-release effect of iodine and the significant antibacterial activity made CS-PVP-I_2-G-M highly potential for applications as a novel natural biomedical sterilization materials. © 2014 Wiley Periodicals, Inc. J. Appl. Polym. Sci. **2015**, *132*, 41797.

KEYWORDS: biomaterials; chitosan; composites with iodine; functionalization of polymers; membranes

Received 4 July 2014; accepted 22 November 2014
DOI: 10.1002/app.41797

INTRODUCTION

As the only basic polysaccharide in nature, chitosan (CS) was obtained by alkaline deacetylation of chitin, containing amino groups, hydroxy groups, oxygen bridge groups, and pyran ring reactive groups with rich electrons. CS therefore has unique physical and chemical properties, as well as distinctive biomedical properties such as biological functionality and compatibility, blood compatibility, security, biodegradability, and so forth,[1–3] all of which make this polymer and its derivatives ideal candidates in the applications of sustained-release carrier as biomedical disinfect materials.[4,5]

As a broad-spectrum fungicide that against most bacteria, fungi, and viruses, iodine showed excellent advantages like high efficiency, low toxicity, cheap, and no drug resistance, and so forth.[6–8] However, the iodine is not stable and difficult to store in a solvent or creams, and the iodine is easily sublimated and decomposed when in use, which could lead to the reduction of effective iodine content, shorten of efficacy time, and difficulties in controlling the dose.[9–11] It will also cause irritation when the iodine is used to the wound directly,[12] therefore a prolonged release of iodine carrier is needed.

A series of investigations on CS[13–15] and its derivatives[16–19] as drug delivery carrier have been performed, according to which CS has been found to play an important role in antibacterial drug delivery, as CS shows no obvious bacteriostatic effect when used as antimicrobial material.[20] Iodine has therefore been tried to be combined with CS to improve its antimicrobial activity of CS antimicrobial material,[21–25] but according to our experiment results and the conclusion of the combined forms between CS and iodine molecules made by Shigeno *et al.*,[21] CS offers slight adsorption to iodine only. The absorption to iodine has been considered to be caused by $n-\delta$ charge transfer between amino groups of CS and iodine molecules. To keep the stability of iodine, the polyvinylpyrrolidone (PVP)–iodine complex has been studied widely as a disinfectant, and has shown potential applications in medicine as a broad spectrum antiseptic, has the bactericidal, fungicidal, sporicidal, protocidal, and virucidal properties.[26–28] Although several iodine-release systems based on iodine incorporated synthetic polymers have been used for water disinfection,[29,30] there was few presentations of the incorporation of small amount of toxic PVP–iodine in natural polysaccharide-based systems for similar applications so far.

Therefore, the PVP was tried to graft onto the CS to improve the charge-transfers and enhance the adsorption of iodine.

In this article, the chitosan grafted polyvinylpyrrolidone gel membrane with iodine (CS-PVP-I_2-G-M) and the intermediate product chitosan–polyvinylpyrrolidone–iodine complex liquid (CS-PVP-I_2-L) was prepared with state-of-the-art methodology. The properties of them were characterized by IR, UV–Vis, SEM, XRD, DSC, particle size analysis, iodine content and releasing regulation of iodine, antibacterial properties, and so forth. The CS-PVP-I_2-G-M could be prepared into various forms of antibacterial, anti-inflammatory medical membrane for medical applications, and the double effects of the sustained-release effect of iodine and the significant antibacterial activity made CS-PVP-I_2-G-M could offer an ideal healing environment for wound surface. The results demonstrated that CS-PVP-I_2-G-M has prospective anti-bacterial and fungal biological properties as medical antibacterial material.

EXPERIMENTAL

Materials

CS (medical grade, with a degree of deacetylation of 90% and molecular weight of 1.32×10^5) was purchased from Zhejiang Golden-Shell Biochemical (China), all other chemicals were at least analytical grade and used as received without further purification. The crop-threatening bacteria (*Staphylococcus aureus* 25922 and *Escherichia coli* 29213) and nutrient broth, and so forth, used for the antimicrobial assay were provided by Hubei Key Laboratory of Bioinorganic Chemistry & Materia Medica; School of Chemistry and Chemical Engineering, Huazhong University of Science and Technology.

Preparation of CS-PVP Emulsion and CS-PVP-I_2-L

CS (10.0 g, 60.0 mmol of pyranose ring) was dissolved in 200 mL acetic acid solution (3 wt %) in a 500 mL three-necked flask, 0.2 g of dimethyl 2,2′-azobis (2-methylpropionate) (AIBME) was added as initiators under the protection of N_2, the solution was stirred under 400 r/min at 80°C for 1.5 h. Forty milliliters of PVP aqueous solution (50 wt %) was added and stirred until a milky white solution was obtained. The solution above was then distillated in a vacuum to about 60 mL, the CS-PVP emulsion was obtained, weighed, and recorded by mg.

The iodine quality required was calculated by the following formula:

$$\frac{x}{m+x+8x+0.05+15}=5\%.$$

x g of I_2 was dissolved in 15 mL ethanol in a 500 mL three-necked flask, $8x$ g of tert-butanol was added under 400 r/min, sodium dodecyl sulfate (0.05 g) was added as surfactant and then stirred for 2 h, the composite solution was added dropwise in the CS-PVP emulsion with a dropping funnel. The CS-PVP-I_2-L was obtained after stirred under 400 r/min at 50°C in water bath for 2 h.

Preparation of CS-PVP Gel Membrane (CS-PVP-G-M) and CS-PVP-I_2-G-M

CS (10.0 g) (45.6 mmol of pyranose ring) was dissolved in 100 mL acetic acid solution (3 wt %) in a three-necked flask, 0.76 g of gelatin was added and then stirred under 400 r/min at 50°C until a uniform phase was reached. A certain amount of CS-PVP emulsion was added and then stirred under 700 r/min for 1 h. The blend was poured into the mold to dry out for 24–36 h at room temperature to obtain the CS-PVP-G-M.

Repeated the steps above, 5 mL, 10 mL, 15 mL, 20 mL, and 25 mL CS-PVP-I_2-L were added into the uniform phase solutions, and then stirred under 700 r/min for 1 h. The blends were poured into the molds to dry out for 24–36 h at room temperature to obtain the CS-PVP-I_2-G-M.

Measurements

The characteristic peaks of CS solution, CS-PVP emulsion, CS-PVP-I_2-L, CS-PVP-G-M, and CS-PVP-I_2-G-M with 25 mL CS-PVP-I_2-L were detected and depicted with AVATAR370 FTIR infrared spectrometer (USA Thermo Nicolet Company). The spectra were recorded in the range of 500–4000 cm^{-1}.

A certain concentration of CS solution, CS-PVP emulsion, CS-PVP-I_2-L, CS-PVP-G-M, and CS-PVP-I_2-G-M with 25 mL CS-PVP-I_2-L was performed under UV irradiation (UV-1601PC UV spectrometer, Shimadzu, Japan) using a medium pressure mercury arc lamp from PrimarcTM UV Technology which provided multiple wavelengths ranging from 200 to 800 nm. The total exposure energy was 2.5 J/cm^2.

The CS-PVP-I_2-L dried out on a clean glass slide, the CS-PVP-G-M and CS-PVP-I_2-G-M were coated with a gold layer with a thickness of 100 μm using an ion sputter coating unit (HITACHI E-1010 ION) for 2 min and observed with a Electron Probe Microanalyzer of Scanning electron microscopy (SEM) (HITACHI S-3400, Japan), under accelerating voltage of 10.0 kV and at magnification of 25.4 mm × 20.0 K.

The particle size distribution and the deviation rate of CS-PVP-I_2-L were tested with a laser particle size analyzer (Malvern Zetasizer Nano ZS, UK) according to the international standards ISO1332l-1996.[31] The CS-PVP-I_2-L was dispersed for 5 min in ultrasonic bath.

The X-ray diffraction (XRD) patterns of CS-PVP-G-M and CS-PVP-I_2-G-M with 25 mL CS-PVP-I_2-L were taken on a BRUKER D2 PHASER X-ray diffractometer with Cu Kα radiation combined with nickel filter operating at 30 kV and 10 mA. The samples were maintained stationary and the scattering angle varied from 5° to 80°, and they were scanned in the reflection mode at a scanning rate of 4°/min.

Various scanning calorimetry investigations of CS-PVP-G-M and CS-PVP-I_2-G-M with 25 mL CS-PVP-I_2-L were performed with a differential scanning calorimeter (PT-10, Linseis, Germany) in aluminum sample pans with heating and cooling at a rate of 20°C/min and scanning over a temperature ranging from 0 to 400°C using nitrogen as the carrier gas.

The iodine content was tested by iodometry, 1.0 g CS-PVP-I_2-G-M with different amounts of CS-PVP-I_2-L was quantitatively weighed in iodine flasks, kept away from light and stirred until the CS-PVP-I_2-G-M turned to be transparent at room temperature after 100 mL calibrated $Na_2S_2O_3$ solution was added. The supernatant was transferred into the basic buret to titrate

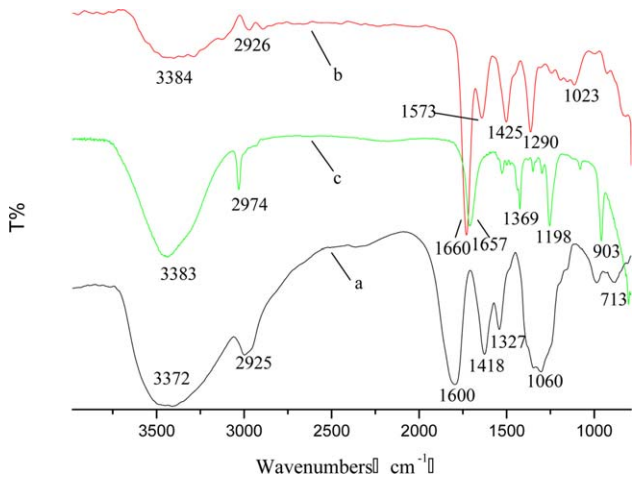

Figure 1. IR spectra of CS solution, CS-PVP emulsion, and CS-PVP-I_2-L. [Color figure can be viewed in the online issue, which is available at wileyonlinelibrary.com.]

25 mL calibrated KIO_3 solution until transparent, with 5 mL KI solution and 5 mL 0.5 mol/L sulfuric acid solution was added, and starch was used as indicator. The formula of iodine content is given below:

$$I2\% = \frac{(C1-C2)\times 0.1}{2m}\times 254\times 100\%,\quad C_{Na_2S_2O_3}$$
$$= \frac{0.025\times C_{KIO_3}\times 6}{V}\qquad C_2 = C_{Na_2S_2O_3},$$

where C_1 is calibrated concentration of sodium thiosulfate (mol/L), V is sodium thiosulfate consumption (mL), m is sample quality.

The releasing regulation of iodine of CS-PVP-I_2-G-M was demonstrated as follows. The samples were cut into square of 4 × 4 cm^2 and immersed in 500 mL pH = 7 simulation buffer solution, stirred slowly at 37°C, 3 mL supernatant was selected at regular intervals for absorbance at 231 nm with the simulation buffer solution as blank sample, and another 3 mL analog exudate was added after each test. The characteristic absorption wavelength of UV–visible spectrophotometer of iodine was tested at 231 nm in simulation buffer solution with pH = 7. The iodine standard curve was depicted after the absorbance of iodine in ethanol solution of different concentrations was tested at 231 nm. The regression equation was obtained at $C = (0.12984 + 12198.17353\ A) \times 10^{-6}$, where C is the concentration of iodine in ethanol solution, A is the absorbance.

$$\text{Formula release } (\%) = \frac{M}{0.0372}\times 100,\ \text{release mass } (M) = C\times 0.25\times 254.$$

Antibacterial activities were investigated using agar well diffusion method, the activity was determined by measuring the diameter of the inhibition zone (in mm). *S. aureus* (as Gram positive bacteria) and *E. coli* (as Gram negative bacteria) were dispersed into the medium, centrifuged pellets of bacteria from a 24 h old culture containing approximately 104–106 CFU (colony forming unit) per mL were spread on the surface of nutrient agar (tryptone 1%, yeast extract 0.5%, NaCl 0.5%, agar 1%, 1000 mL of distilled water, pH = 7.0), which was autoclaved under 121°C for at least 20 min. Wells were created in medium with the help of a sterile metallic bores and then cooled down to 45°C. The bacteria concentration of about 1.08 × 10^5 cells/L, 30 mL of the solution diluted 10-fold mounted to a Petri dish of 12 cm diameter in the cooled and solidified. The CS-PVP-G-M and the CS-PVP-I_2-G-M with different amounts of CS-PVP-I_2-L having a diameter of 10 mm of the wafer, UV sterilized 30 min, respectively, attached to different locations in the dish, the plates were kept for incubation at 37°C for 24 h and then the plates were checked for the formation of zone of inhibition. Each inhibition zone was measured three times by caliper to get an average value. Inhibition zone diameter was recorded afterwards.[32]

RESULTS AND DISCUSSION

FTIR Characterization of CS Solution, CS-PVP Emulsion, and CS-PVP-I_2-L

First, the strong broad absorption peak around 3372 cm^{-1} of CS solution [Figure 1(a)] should be assigned to the stretching vibration of OH and NH, and the intermolecular hydrogen bonds of the polysaccharide. The absorption peak at 2925 cm^{-1} was due to —CH_2— stretching vibration, and the strong absorption peaks at 1600 cm^{-1} corresponding to aromatic carbon rings and amide II, which indicated that CS had a high deacetylation degree.[32] The absorption peak at 1418 cm^{-1} was due to the asymmetric bending vibration of NH_3^+, the absorption peak at 1327 cm^{-1} was due to the C—H in-plane bending vibration, and the strong absorption peaks at 1130, 1060, and 713 cm^{-1} which were characteristic peaks of the saccharide structure.[30]

Second, in comparison with the CS, the grafting of PVP on CS made the absorption peak at 3372 cm^{-1}, as the OH and NH stretching vibration of CS-PVP emulsion [Figure 1(b) red line] moved to 3384 cm^{-1}. The absorption peak of aromatic carbon rings and C=O stretching vibration became stronger and the red line shifted to 1660 cm^{-1}. The new absorption peak occurred at 1573 cm^{-1} was assigned to the absorption peak of tertiary amino and —C=O symmetric contraction vibration. The absorption peak at 1327 cm^{-1} was because the C—H

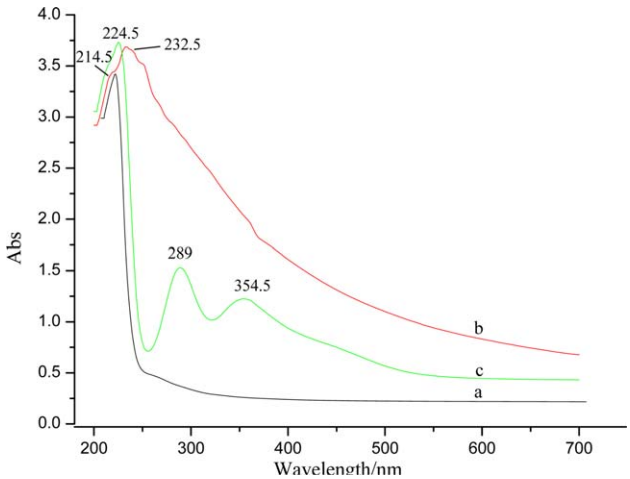

Figure 2. UV–Vis spectra of CS solution, CS-PVP emulsion, and CS-PVP-I_2-L. [Color figure can be viewed in the online issue, which is available at wileyonlinelibrary.com.]

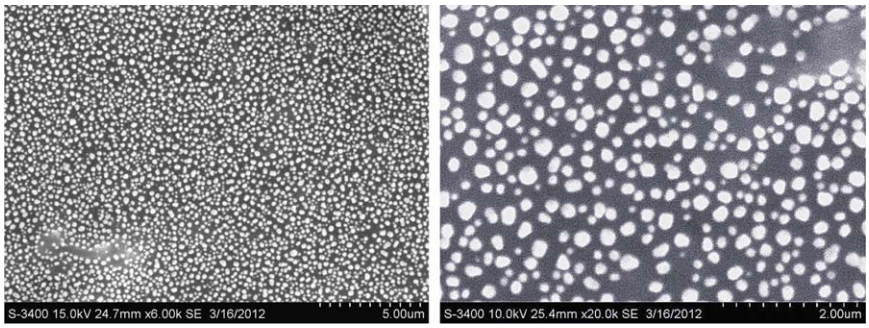

Figure 3. SEM image of CS-PVP-I_2-L. [Color figure can be viewed in the online issue, which is available at wileyonlinelibrary.com.]

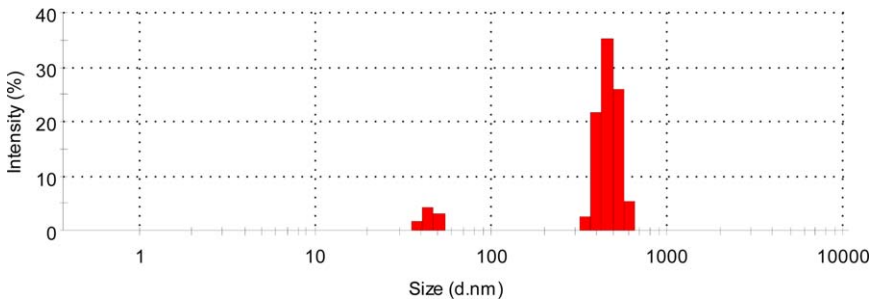

Figure 4. Particle size distribution of CS-PVP-I_2-L. [Color figure can be viewed in the online issue, which is available at wileyonlinelibrary.com.]

in-plane bending vibration disappeared. The new absorption peak appeared at 1290 cm^{-1} was due to the absorption peak of the C—N stretching vibration of PVP and CS derivatives. PVP is therefore have grafted onto CS.

Further, the absorption peak intensity at 3383 cm^{-1} assigned to NH and OH stretching vibration was enhanced after the CS-PVP emulsion adsorbed the iodine, and the absorption peak intensity at 2970 cm^{-1} was due to C—H symmetric stretching vibration of methyl and hence enhanced methine. At the same time, the absorption peak at 1573 cm^{-1} was caused by the vibration of tertiary amino and —C═O symmetric contraction disappeared. The new absorption peak occurred at 1369 cm^{-1} which was due to C—H symmetry bending vibration of methyl, and the new absorption peak appeared at 1198 cm^{-1} was caused by the stretching vibration of C—O, C—N, and C—C. The strong absorption peak occurred at 903 cm^{-1} was the result of the plane bending vibration of C—H. All the results showed that the iodine had an influence on the CS-PVP emulsion, which was due to the dipole moment changed by intermolecular hydrogen bonds.

UV–Vis Spectroscopy of CS Solution, CS-PVP Emulsion, and CS-PVP-I_2-L

According to the comparison of the UV–vis spectroscopy of CS solution, CS-PVP emulsion, and CS-PVP-I_2-L (Figure 2), a strong single characteristic peak appeared at 214.5 nm of CS solution [Figure 2(a)], and there was low absorption between 240 and 700 nm. After PVP had been grafted onto CS, the strong single characteristic peaks turned to be widened and the red line moved to 232.5 nm, hence the high absorption between 240 and 700 nm of CS-PVP emulsion [Figure 2(b)].

Compared with the CS-PVP emulsion, the CS-PVP-I_2-L [Figure 2(c)] had two weak absorption peaks at 289 nm and 354.5 nm, respectively, a strong absorption peaks at 224.5 nm, which was due to the increased $n \rightarrow \sigma^*$ transition of CS-PVP molecules caused by the absorption of iodine.

SEM Observation of CS-PVP-I_2-L

The CS-PVP-I_2 complex liquid dried out and was then observed with SEM (Figure 3), the iodine in copolymer macromolecules

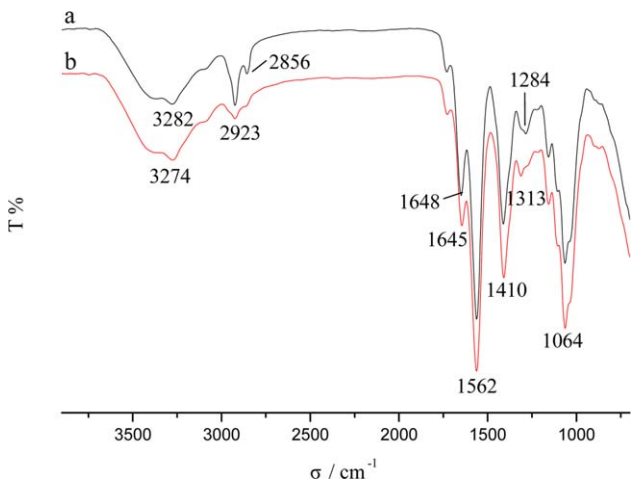

Figure 5. IR spectra of CS-PVP-G-M (a) and CS-PVP-I_2-G-M (b) with 25 mL CS-PVP-I_2-L. [Color figure can be viewed in the online issue, which is available at wileyonlinelibrary.com.]

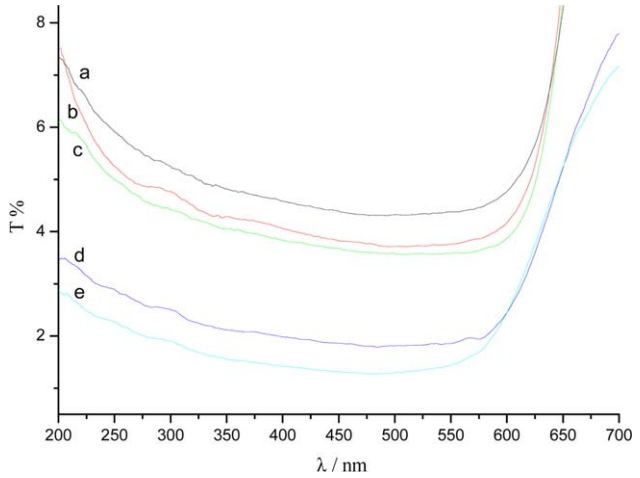

Figure 6. UV–Vis spectra of CS-PVP-I_2-G-M with different amounts of CS-PVP-I_2-L (a): 5 mL, (b): 10 mL, (c): 15 mL, (d): 20 mL, and (e): 25 mL. [Color figure can be viewed in the online issue, which is available at wileyonlinelibrary.com.]

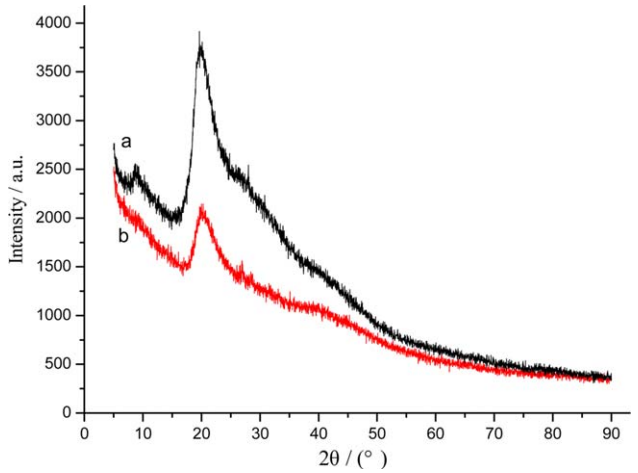

Figure 8. XRD patterns of CS-PVP-G-M (a) and CS-PVP-I_2-G-M (b) with 25 mL CS-PVP-I_2-L. [Color figure can be viewed in the online issue, which is available at wileyonlinelibrary.com.]

showed a spherical structure, that the size of iodine microspheres was uniform, and the iodine sphere showed less aggregation. In addition, the spherical was regular with round surface, showed a good dispersibility in the CS-PVP copolymer macromolecules, which was because the grafted hydrophobic groups increased the repulsion between the molecular chains in the course of graft and copolymerization. This kind of repulsion made the iodine molecules uniformly dispersed in the CS chain molecule, indicated the CS-PVP copolymer has a strong stability of iodine.

Laser Particle Size Analysis of CS-PVP-I_2-L

As it can be seen from the particle size distribution of CS-PVP-I_2-L (Figure 4), the CS-PVP-I2 complex was mainly distributed in the regions of 38–51 nm and 342–615 nm, where the deviation rate was 0.681. The region between 38 and 51 nm was probable particle size of I*n*- ($n = 3, 5, 7, 9\ldots$), due to the volatility of iodine molecules. And the region between 342 and 615 nm was CS-PVP-I_2 complex. The results showed iodine molecule was stable and uniformly dispersed in the copolymer molecule in nano form to some extent.

Obviously, the nano form to some extent of iodine has the properties of nanomaterials, like the surface effect which leads to a large specific surface area, it increases rapidly along with decreasing particle size. On one hand, the surface effect enhances dispersion and stability of the iodine and the complexing ability of copolymers molecule groups on iodine. All the characteristics made CS-PVP-I_2 complex has a strong bactericidal effect which could kill bacteria and viruses.

IR Spectra of CS-PVP-G-M and CS-PVP-I_2-G-M

The IR spectral absorption peak at 3282 cm^{-1} of CS-PVP-G-M [Figure 5(a)] was due to the stretching vibration of OH and NH, and the intermolecular hydrogen bonds of the polysaccharide. The absorption peaks at 2923 cm^{-1} and 2856 cm^{-1} were the results of the stretching vibration of —CH_3 and —CH_2—, respectively. The absorption peak at 1648 cm^{-1} was due to amide I of PVP and the polysaccharide, while the absorption peaks at 1562 cm^{-1} and 1313 cm^{-1} were caused by amide II and amide III, respectively. The absorption peak at 1410 cm^{-1} was due to the C—N stretching vibration of primary amide, the absorption peak at 1064 cm^{-1} was the result of the C—O—C stretching vibration of sugar ring.

In comparison with the CS-PVP-G-M, the absorption peak of CS-PVP-I_2-G-M [Figure 5(a)] was caused by OH and NH stretching vibration blue which moved from 3282 cm^{-1} to 3274 cm^{-1}, and the absorption peak at 2923 cm^{-1} and 2856 cm^{-1} was due to —CH_3 and —CH_2— stretching vibration weakened and disappeared, indicated that the iodine molecule

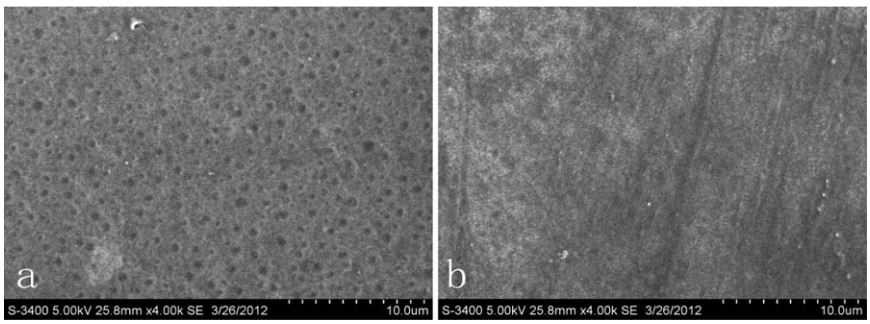

Figure 7. SEM image of CS-PVP-G-M (a) and CS-PVP-I_2-G-M (b).

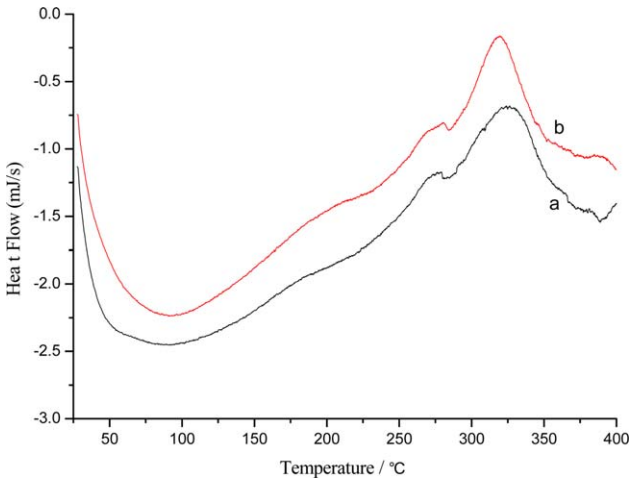

Figure 9. DSC patterns of CS-PVP-G-M (a) and CS-PVP-I_2-G-M (b) with 25 mL CS-PVP-I_2-L. [Color figure can be viewed in the online issue, which is available at wileyonlinelibrary.com.]

had an impact on the molecular structure of copolymer after absorbed by the CS-PVP groups.

UV–Vis Spectra of CS-PVP-I_2-G-M with Different Amounts of CS-PVP-I_2-L

As it can be seen from the UV–Vis spectra of CS-PVP-I_2-G-M (Figure 6), the absorbance increased along with the increasing amounts of CS-PVP-I_2-L at 200–600 nm. The transmittances of CS-PVP-I_2-G-M were between 4 and 6%, when the amounts of CS-PVP-I_2-L were 5 mL, 10 mL, and 15 mL, respectively. The CS-PVP-I_2-G-M showed lower transmittance, when the amounts of CS-PVP-I_2-L were 20 mL and 25 mL, were 2–3%, respectively.

All the phenomena above were triggered by the fact that the increased amounts of CS-PVP-I_2-L darkened the color of the membrane, leading to the strong absorption between 200 and 600 nm and reducing the transmittance, which indicated that the iodine can be well adsorbed in the CS-PVP polymer.

SEM Analysis of CS-PVP-G-M and CS-PVP-I_2-G-M

Microstructures of the CS-PVP-G-M surface [Figure 7(a)] and CS-PVP-I_2-G-M surface [Figure 7(b)] were investigated by SEM. The CS-PVP-G-M has an uneven surface, many depression holes were presented, which was may be caused by the copolymer repulsion between the molecular chains because of the existence of hydrophobic groups in the process of graft copolymerization reaction.

The CS-PVP-I_2-G-M surface [Figure 7(b)] tended to blend flat and smooth compared with CS-PVP-G-M surface, showed good dispersibility, which was probably due to the excellent complexation (adsorption) ability of iodine on the polymer of CS-PVP, indicated a good compatibility between each component of CS-PVP-I_2-G-M.

XRD Analysis of CS-PVP-G-M and CS-PVP-I_2-G-M

The sharp diffraction peak at 20° of CS-PVP-G-M [Figure 8(a)] was due to the characteristic peak of CS and PVP according to the XRD pattern analysis, and the weak diffraction peaks at 8° was due to the characteristic peak of amino-acetylated CS, where the remote areas were non-crystalline regions.[33] The CS-PVP-I_2-G-M results showed a good crystallinity, large grains, as well as orderly arranged internal atoms.

In comparison with the CS-PVP-G-M, the diffraction intensity of CS-PVP-I_2-G-M [Figure 8(b)] at 20° was weakened, and the characteristic peak of *N*-acetylation at 8° was disappeared, with lowered crystallinity. This was caused by the occurred crystals defects due to the position of iodine in the unit cell, which damaged the integrity of the crystals weakening the diffraction peaks. That also might because that several internal stress within the range of grain and internal stress within the atomic range reduced the diffraction intensity of CS-PVP-I_2-G-M. All these assumptions above indicated that the iodine had an impact on the molecular structure and the spatial structure of the copolymer membrane.

DSC Analysis of CS-PVP-G-M and CS-PVP-I_2-G-M

An endothermic peak emerged at 90.3°C seen according to the DSC pattern analysis of the CS-PVP-I_2-G-M [Figure 9(a)], and two exothermic peaks appeared at 285.5°C and 326.1°C, respectively. The exothermic peak at 326.1°C showed a dramatic change of the red line, the glass transition temperature was thus 326°C, and the enthalpy change was 97.02 J/g. The CS-PVP-I_2-G-M [Figure 9(b)] had an endothermic peak at 92.4°C, and two exothermic peaks at 280.4°C and 319.4°C, respectively, where the most obvious exothermic peak occurred at 319.4°C, which was the glass transition temperature, and the enthalpy change was 71.26 J/g.

In comparison with the CS-PVP-G-M, the glass transition temperature of CS-PVP-I_2-G-M decreased to 319.4°C, this was because that the reaction between iodine molecule and the groups of the copolymer molecules damaged the interaction between the molecular chains and the intermolecular hydrogen bonds, reducing the intermolecular crystallinity, which indicated that the iodine was well adsorbed in the groups of the polymer chain. The experiment results were coherent with the XRD results.

Iodine Content Determination of CS-PVP-I_2-G-M

According to the iodine content measurement results, the iodine content of CS-PVP-I_2-G-M (Table I) increased along with the increasing amounts of CS-PVP-I_2-L, showing an upward tendency. The mass fraction of iodine was 20.98% and the volume

Table I. Iodine Content of CS-PVP-I_2-G-M Along with the Added Volumes of CS-PVP-I_2-L

The volume added of CS-PVP-I_2 complex liquid	5 mL	10 mL	15 mL	20 mL	25 mL
I_2 (%)	4.41	8.11	12.02	16.46	20.98

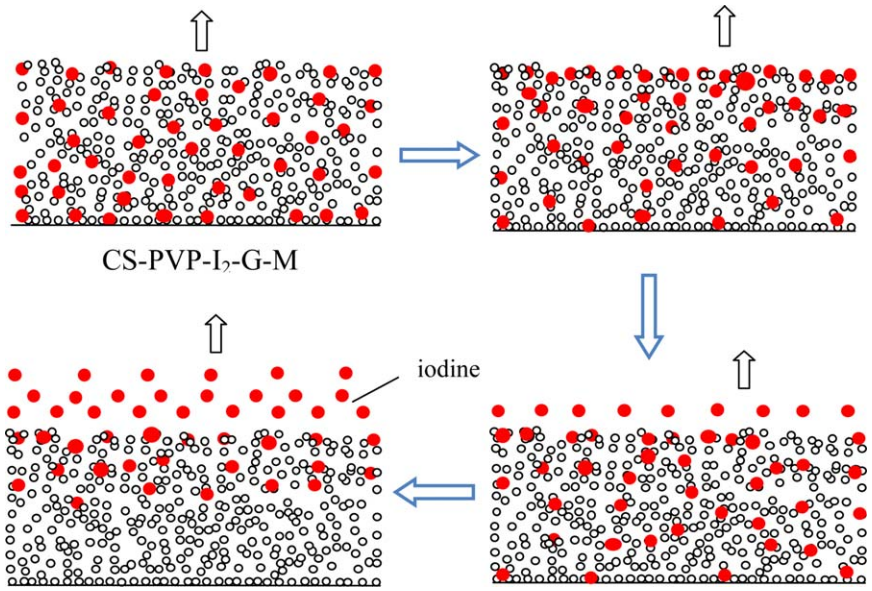

Figure 10. The iodine release schematic of CS-PVP-I_2-G-M. [Color figure can be viewed in the online issue, which is available at wileyonlinelibrary.com.]

of CS-PVP-I_2-L added was 25 mL, which indicated that the CS-PVP polymer had a good adsorption of iodine. It was because that the pyrrole rings of polyvinyl pyrrolidone in the polymer increased the absorption of iodine molecules.

The Iodine Release Schematic of CS-PVP-I_2-G-M

When the CS-PVP-I_2-G-M released iodine in the simulated buffer solution, the release process could be simulated using the release kinetic model—Fick diffusion laws, we have established a model release like Figure 10, under normal conditions, the surface of the carrier material CS-PVP-I_2-G-M absorbed a large number of iodine, the iodine release of the CS-PVP-I_2-G-M surface first will has a burst effect, and then spread. It was assumed that the release of iodine firstly occurred on the surface of the membrane, then inside the membrane.[4,5]

In addition, the effect of slow controlled release of iodine not only can reduce the stimulations of the skin or wound surface using iodine directly, but also could keep the iodine retained in the skin or wound surface longer, and therefore enhanced inhibitory effect. CS also has effect on bleeding, inflammation, and tissue repair on human trauma. The double effects of CS and iodine provide an ideal healing environment for wound surface.

Iodine Release of CS-PVP-I_2-G-M in the Simulated Buffer Solution

The releasing rule of CS-PVP-I_2-G-M (Figure 11) in the simulated buffer solution showed that the emissions of iodine increased along with the iodine content increases. There was a rapid release within a short time, and the maximum release of iodine was obtained at about 90 min. After the maximum release was reached, the releases of iodine decreased to a certain concentrations and reached a balance. This was because that the release of iodine firstly occurred on the surface of the membrane, then inside the membrane, thus the release rate decreased and remained steady,[24] which are coherent with the predictions of the iodine release schematic.

In addition, the emission of iodine was maintained within a certain range and kept at a stable level for a long time, there were still no apparent downtrends at 800 min. The maximum release of iodine remained at about 1.23%, when the volume of CS-PVP-I_2-L added was 25 mL, and the emission of iodine was 0.79% at 1440 min. These results above indicated that the CS-PVP polymer not only had a good adsorption of iodine, but also had a sustained-release effect of iodine and a stable emission when made into membrane materials. The properties above made CS-PVP-I_2-G-M great potential as medical materials that sustained-release of iodine.

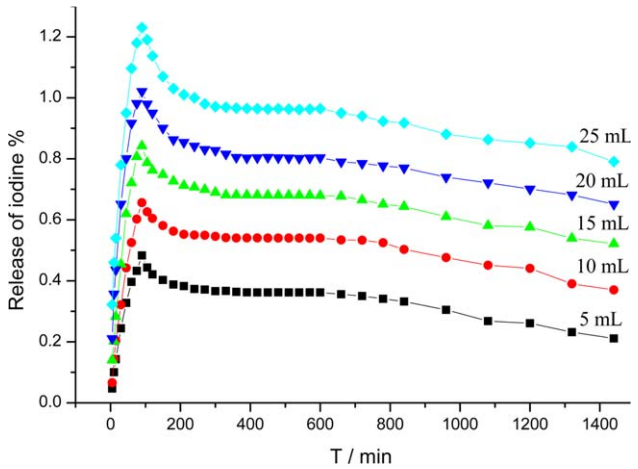

Figure 11. Iodine release of CS-PVP-I_2-G-M in the simulated buffer solution. [Color figure can be viewed in the online issue, which is available at wileyonlinelibrary.com.]

Table II. Inhibition Indices of CS-PVP-G-M and CS-PVP-I_2-G-M with Different Volume of CS-PVP-I_2-L Against *S. aureus* and *E. coli*

	Inhibition zone (mm)	
Samples	*E. coli*	*S. aureus*
CS-PVP-G-M	8 ± 1	9 ±1
CS-PVP-I_2-G-M (5 mLCS-PVP-I_2-L)	16 ± 1	18 ± 1
CS-PVP-I_2-G-M (10 mL CS-PVP-I_2-L)	22 ± 1	28 ± 1
CS-PVP-I_2-G-M (15 mL CS-PVP-I_2-L)	25 ± 1	30 ± 1
CS-PVP-I_2-G-M (20 mL CS-PVP-I_2-L)	28 ± 1	33 ± 1
CS-PVP-I_2-G-M (25 mL CS-PVP-I_2-L)	31 ± 1	36 ± 1

Antibacterial Properties of CS-PVP-G-M and CS-PVP-I_2-G-M

According to the standard of antibiotic sensitivity: when the inhibition zone diameter < 10 mm, the drug sensitivity is resistance; 10–15 mm, is moderately sensitive; >15 mm, is highly sensitive. The antibacterial activity of the CS-PVP-G-M and CS-PVP-I_2-G-M with different mass fraction of iodine was tested by the method of measuring the diameter of the inhibition zone (Table II). The inhibition zone diameters of CS-PVP-G-M against *S. aureus* and *E. coli* were (9 ± 1) mm and (8 ± 1) mm, respectively, showed little bacteriostasis effect. The inhibition zone diameters of CS-PVP-I_2-G-M with different amounts of CS-PVP-I_2-L against *S. aureus* and *E. coli* were both greater than 16 mm, which indicated a palpable antibacterial activity. Besides, the bacteriostatic level of CS-PVP-I_2-G-M against *S. aureus* and *E. coli* increased along with the increase of iodine content. Compared with the CS-PVP-G-M, the CS-PVP-I_2-G-M has an observable improvement of antibacterial activity.

Moreover, the CS-PVP-I_2-G-M was more active against the *S. aureus* than against the *E. coli*. The different inhibition zone diameters of *S. aureus* and *E. coli* could be attributed to their different cell wall.[24] Therefore, the ATU-HPCS-I_2-M has different effects on the two kinds of bacteria. And the inhibition zone diameters of CS-PVP-I_2-G-M against *S. aureus* and *E. coli* were (36 ± 1) mm and (31 ± 1) mm, respectively, when the volume of CS-PVP-I_2-L added was 25 mL. The results above prove the excellent antimicrobial activity of the prepared CS-PVP-I_2-G-M, made it hold great potential as antibacterial material that prevents the most bacteria.

CONCLUSIONS

The CS-PVP-I_2-L and the CS-PVP-I_2-G-M were prepared successfully in this work. The particle size distribution results showed that the CS-PVP-I_2 complex were mainly distributed in the regions of 38–51 nm and 342–615 nm, and the deviation rate was 0.681. The results of UV of the CS-PVP-I_2-G-M showed a strong absorption between 200 and 600 nm. The glass transition temperature of the CS-PVP-I_2-G-M was 319°C. The iodine release showed that the emission of iodine was maintained within a certain range and kept at a stable level for a long time, and has a sustained-release effect of iodine. The CS-PVP-I_2-G-M demonstrated significant antibacterial activity compared with the CS-PVP-G-M against *S. aureus* and *E. coli*. Double effects sustained-release effect of iodine and the significant antibacterial activity made CS-PVP-I_2-G-M highly potential for further research as a medical antibacterial materials.

ACKNOWLEDGMENTS

The authors show greatly appreciation for the financial support from the fund of National Undergraduate Innovative Training Program (201310856012) and the fund of Graduate research and innovation projects (E1-0903-14-01112), also express sincere thanks to the teacher An Ding from Tongji University for the assistance in performing modify paper grammars and the constructive suggestions of my teachers and the reviewers.

REFERENCES

1. Bordenave, N.; Grelier, S.; Coma, V. *Biomacromolecules* **2009**, *11*, 88.
2. Mathews, S.; Kaladhar, K.; Sharma, C. P. *J. Biomed. Mater. Res. Part A* **2006**, *79*, 147.
3. Jae, H. P.; Yong, W. C.; Hesson, C.; Ick, C. K.; Seo, Y. *J. Biomacromolecules* **2003**, *4*, 1087.
4. Richard, J.; Chen, B. Q. *Carbohydr. Polym.* **2014**, *103*, 70.
5. Said, E.; Khaled, D. K.; Maher, Z. E.; Mohamed, E. *J. Appl. Polym. Sci.* **2007**, *103*, 1651.
6. Morales-Fernández, L.; Fernández-Crehuet, M.; Espigares, M.; Moreno, E.; Espigares, E. *Eur. J. Clin. Microbiol. Infect. Dis.* **2014**, *33*, 103.
7. Drakovi, R. S.; Bzeni, J.; Ratkovi, M.; Drakovi, R. J. *Isotopes Environ. Health Stud.* **1974**, *10*, 290.
8. Reverdy, M. E.; Surgot, M.; Fleurette, J.; Mouren, C. *Pathol. Biol.* **1983**, *31*, 551.
9. Weinstabl, A.; Amann, P. M.; Wurpts, G.; Merk, H. F. *J. Dtsch. Dermatol. Ges.* **2012**, *10*, 865.
10. Atwater, J. E.; Sauer, R. L.; Schultz, J. R. *J. Environ. Sci. Health Part A* **1996**, *31*, 1965.
11. Hans, B. *Best Pract. Res. Clin. Endocrinol. Metab.* **2010**, *24*, 107.
12. Leung, A. M.; Braverman, L. E. *Nat. Rev. Endocrinol.* **2014**, *10*, 136.
13. Paul, W.; Sharma, C. P. *STP Pharm. Sci.* **2000**, *10*, 5.
14. Yoshino, T.; Machida, Y.; Onishi, H.; Nagal, T. *Drug. Dev. Ind. Pharm.* **2003**, *29*, 417.
15. Lv, Y.; Huang, H. L.; Yang, B. H.; Liu, H.; Li, Y. P.; Wang, J. Y. *Carbohydr. Polym.* **2014**, *111*, 101.
16. Huang, W.; Wang, Y. J.; Zhang, S.; Huang, L.; Hua, D. B.; Zhu, X. L. *Macromolecules* **2013**, *46*, 814.
17. Risbud, M. V.; Hardikar, A. A.; Bhat, S. V.; Bhonde, R. R. *J. Control. Release* **2000**, *68*, 23.
18. Kitae, R.; Kyunghwan, K.; Tae-il, K. *Macromol. Res.* **2014**, *22*, 264.
19. Don, T. M.; King, C. F.; Chiu, W. Y. *J. Appl. Polym. Sci.* **2002**, *86*, 3057.
20. Foster, L. J. R.; Julian, B. *Biotechnol. Lett.* **2011**, *33*, 417.
21. Shigeno, Y.; Kondo, K.; Takemoto, K. *Die Angew. Makromol. Chem.* **1980**, *91*, 55.
22. Shigeno, Y.; Kondo, K.; Takemoto, K. *Die Angew. Makromol. Chem.* **1981**, *182*, 709.

23. Shigeno, Y.; Kondo, K.; Takemoto, K. *J. Appl. Polym. Sci.* **1980**, *25*, 731.
24. Sai, M. Z.; Zhong, S. L.; Tang, Y.; Ma, W. T.; Sun, Y. G.; Ding, D. R. *J. Appl. Polym. Sci.* **2014**, 131.
25. Chen, S. P.; Wang, Y. T. *J. Appl. Polym. Sci.* **2001**, *82*, 2414.
26. Berkelman, R. L.; Holland, B. W.; Anderson, R. L. *J. Clin. Microbiol.* **1982**, *25*, 635.
27. Arakeri, G.; Brennan, P. A. *Int. J. Oral Max. Surg.* **2011**, *40*, 173.
28. Birnbaum, L. M.; Hopp, D. D.; Merteus, B. F. *Plast. Reconstr. Surg.* **1982**, *69*, 956.
29. Punyani, S.; Narayanan, P.; Vasudevan, P.; Singh, H. *J. Appl. Polym. Sci.* **2007**, *103*, 3334.
30. Tyagi, M.; Singh, H. *J. Appl. Polym. Sci.* **2000**, *76*, 1109.
31. ISO13321—1996. Particle size analysis—photon correlation spectroscopy. Available at: http://fjour.blyun.com/views/specific/3004/FStdDetail.jsp?dxNumber=320101542807&d=D509684B9D171086F25BD50B6A64A3C0.
32. Nadia, A. M.; Nahed, A. *Cellulose* **2012**, *19*, 1879.
33. Li, Q. L.; Chen, Z. Q.; Darvell, B. W.; Liu, L. K.; Jiang, H. B.; Zen, Q.; Peng, Q.; Ou, G. M. *J. Biomed. Mater. Res. Part B* **2007**, *82*, 481.